List of Supplementary Materials

Fig. S1 to Fig S4

Table S1 and S2

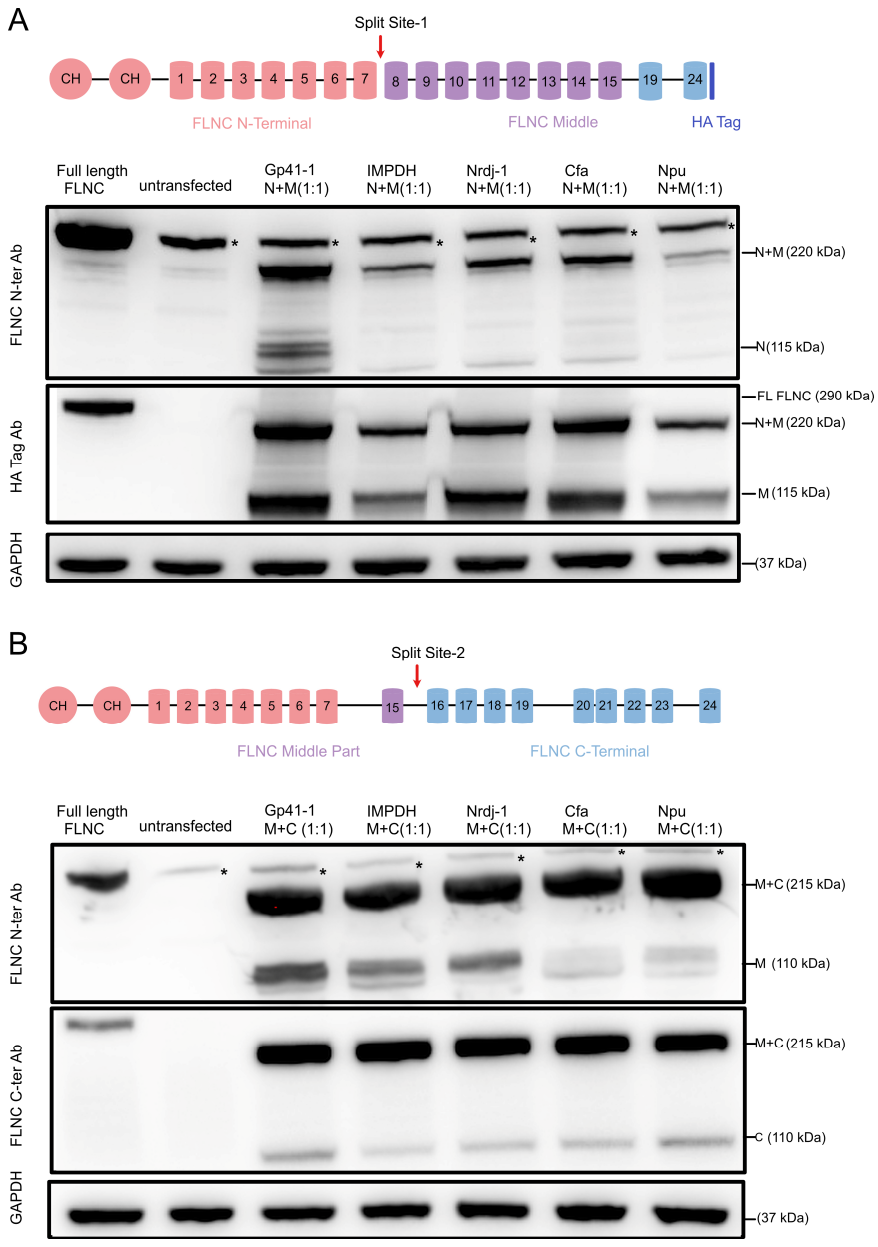


Fig. S1. Screening strategy for candidate split-intein pairs at the two FLNC junctions.
(A) Partial FLNC constructs used to evaluate the Ig7–Ig8 junction. HEK293 cells were cotransfected at a 1:1 ratio with FLNC-N and FLNC-M junction-screening constructs fused to the indicated split-intein halves. The constructs were designed only to test the junction and did not encode the complete full-length FLNC sequence. Reconstituted N+M products and individual fragments were detected with antibodies against the FLNC N terminus and HA tag. Asterisks indicate non-specific bands.
(B) Partial FLNC constructs used to evaluate the Ig15–Ig16 junction. HEK293 cells were cotransfected at a 1:1 ratio with FLNC-M and FLNC-C junction-screening constructs fused to the indicated split-intein halves. Reconstituted M+C products and individual fragments were detected with antibodies against the FLNC N- and C-terminal regions. Asterisks indicate non-specific bands. GAPDH served as a loading control. Blots are representative of at least three independent experiments.

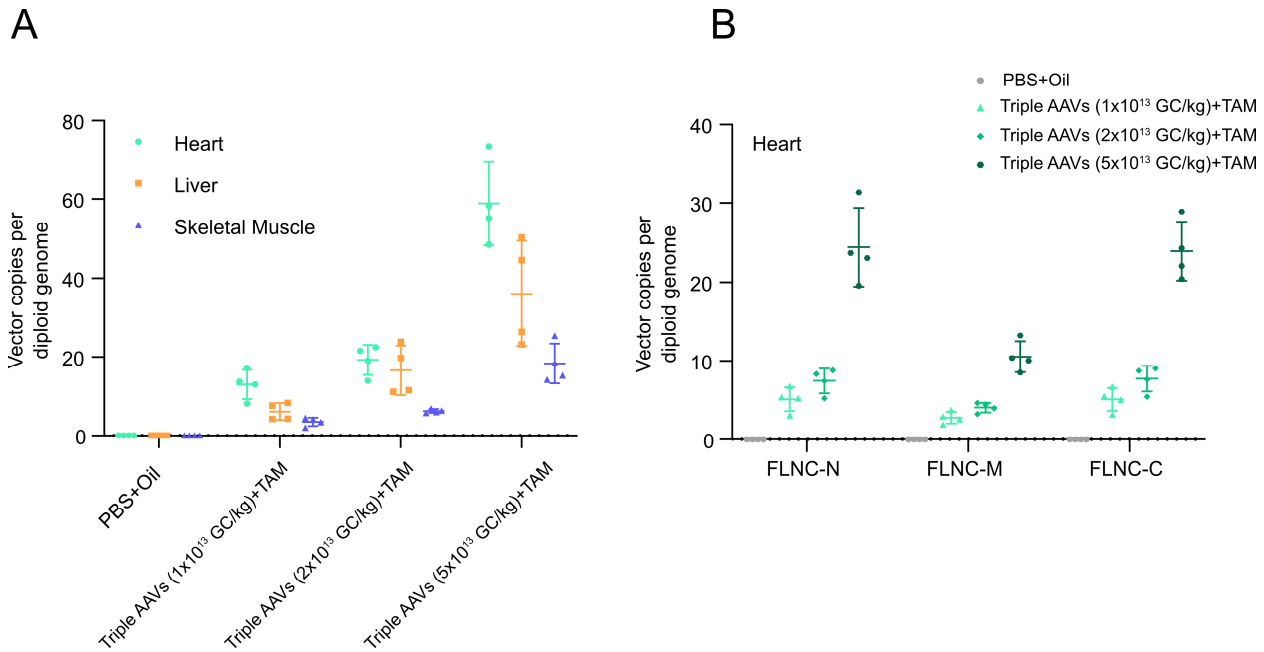


Fig. S2. Tissue distribution of vector genomes after systemic triple-AAV delivery.
(A) Vector genome copies per diploid genome in heart, liver, and skeletal muscle from PBS+Oil controls and *Flnc*-iCKO mice treated with triple AAVs at total doses of 1×10^{13}, 2×10^{13}, or 5×10^{13} GC/kg before tamoxifen administration.
(B) Vector genome copies of individual FLNC-N, FLNC-M, and FLNC-C AAV vectors in heart tissue from PBS+Oil control and triple-AAV-treated *Flnc*-iCKO mice. All three vectors were detected in the heart across the tested doses. Each dot represents one mouse; horizontal bars indicate the mean (n = 4 mice per group).

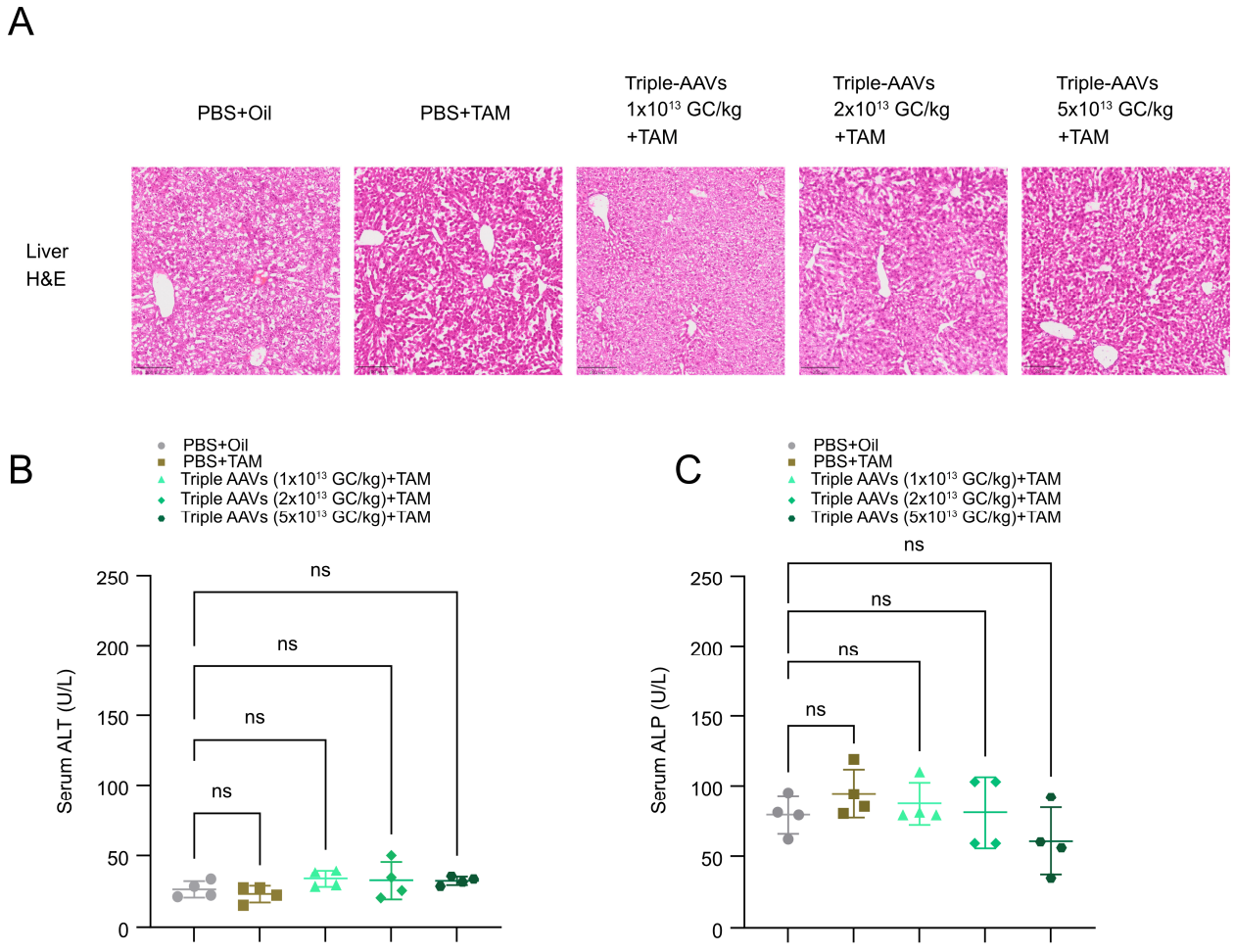


Fig. S3. Liver histology and serum biochemical analysis after systemic triple-AAV delivery.
(A) Representative H&E-stained liver sections from PBS+Oil controls, PBS+TAM *Flnc*-iCKO mice, and *Flnc*-iCKO mice treated with triple AAVs at 1 × 10^{13}, 2 × 10^{13}, or 5 × 10^{13} GC/kg before tamoxifen administration. Scale bars, 200 μm. Images are representative of four mice per group.
(B and C) Serum alanine aminotransferase (ALT) (B) and alkaline phosphatase (ALP) (C) activities measured 20 weeks after AAV administration. Each dot represents one mouse, and horizontal bars indicate the mean (n = 4 mice per group). Statistical significance was assessed by one-way ANOVA followed by Dunnett's multiple-comparisons test comparing each indicated group with the PBS+TAM group. NS, not significant.

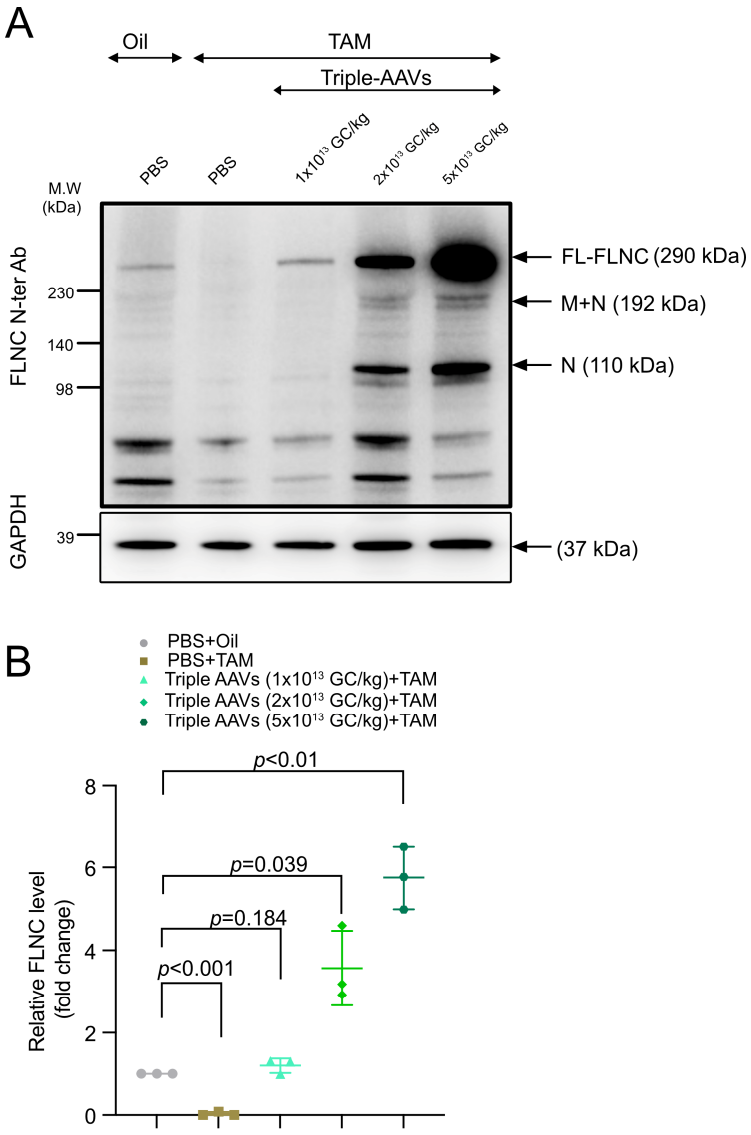


Figure S4. N-terminal FLNC immunoblotting confirms dose-dependent full-length FLNC reconstitution following triple-AAV treatment.
(A) Representative Western blot of ventricular lysates using an antibody against the N terminus of FLNC. Full-length FLNC (FL-FLNC; ~290 kDa), N-terminal–plus–middle (N+M; ~192 kDa), and N-terminal (N; ~110 kDa) products are indicated. GAPDH served as a loading control. Samples are from PBS+Oil, PBS+TAM, and Triple-AAV–treated mice at the indicated total vector doses (1×10^{13}, 2×10^{13}, and 5×10^{13} GC/kg).
(B) Quantification of full-length FLNC protein levels detected with the N-terminal antibody. FLNC band intensities were normalized to GAPDH and expressed relative to the PBS+Oil control on the corresponding blot, which was set to 1. Data are shown as mean ± SD; each symbol represents 1 mouse (n = 3 mice per group). Normalized fold-change values for PBS+TAM and each Triple-AAV treatment group were compared with the PBS+Oil reference value of 1 using one-sample t tests. P values are indicated in the graph.

68
69

70 **Supplementary Table 1. List of plasmids used in this study**

Construct	Description
FLFLNC-N	CMV-driven expression construct encoding the FLNC N-terminal fragment followed by the N-terminal half of the GP41-1 split intein; used in Fig. 1.
FLFLNC-M	CMV-driven expression construct encoding the C-terminal half of the GP41-1 split intein, followed by the FLNC middle fragment and the N-terminal half of the IMPDH split intein; used in Fig. 1.
FLFLNC-C	CMV-driven expression construct encoding the C-terminal half of the IMPDH split intein followed by the FLNC C-terminal fragment; used in Fig. 1.
FCE1N	CMV-driven expression construct encoding the FLNC N-terminal fragment followed by the N-terminal half of the GP41-1 split intein; used in Supplementary Fig. S1A.
FCE2N	CMV-driven expression construct encoding the FLNC N-terminal fragment followed by the N-terminal half of the IMPDH split intein; used in Supplementary Fig. S1A.
FCE3N	CMV-driven expression construct encoding the FLNC N-terminal fragment followed by the N-terminal half of the Nrdj-1 split intein; used in Supplementary Fig. S1A.

FCE4N	CMV-driven expression construct encoding the FLNC N-terminal fragment followed by the N-terminal half of the Cfa split intein; used in Supplementary Fig. S1A.
FCE5N	CMV-driven expression construct encoding the FLNC N-terminal fragment followed by the N-terminal half of the Npu split intein; used in Supplementary Fig. S1A.
FCE1M	CMV-driven expression construct encoding the C-terminal half of the GP41-1 split intein followed by the FLNC middle fragment; used in Supplementary Fig. S1A.
FCE2M	CMV-driven expression construct encoding the C-terminal half of the IMPDH split intein followed by the FLNC middle fragment; used in Supplementary Fig. S1A.
FCE3M	CMV-driven expression construct encoding the C-terminal half of the Nrdj-1 split intein followed by the FLNC middle fragment; used in Supplementary Fig. S1A.
FCE4M	CMV-driven expression construct encoding the C-terminal half of the Cfa split intein followed by the FLNC middle fragment; used in Supplementary Fig. S1A.
FCE5M	CMV-driven expression construct encoding the C-terminal half of the Npu split intein followed by the FLNC middle fragment; used in Supplementary Fig. S1A.

FCMB1M	CMV-driven expression construct encoding the FLNC middle fragment followed by the N-terminal half of the GP41-1 split intein; used in Supplementary Fig. S1B.
FCMB2M	CMV-driven expression construct encoding the FLNC middle fragment followed by the N-terminal half of the IMPDH split intein; used in Supplementary Fig. S1B.
FCMB3M	CMV-driven expression construct encoding the FLNC middle fragment followed by the N-terminal half of the Nrdj-1 split intein; used in Supplementary Fig. S1B.
FCMB4M	CMV-driven expression construct encoding the FLNC middle fragment followed by the N-terminal half of the Cfa split intein; used in Supplementary Fig. S1B.
FCMB5M	CMV-driven expression construct encoding the FLNC middle fragment followed by the N-terminal half of the Npu split intein; used in Supplementary Fig. S1B.
FCMB1C	CMV-driven expression construct encoding the C-terminal half of the GP41-1 split intein followed by the FLNC C-terminal fragment; used in Supplementary Fig. S1B.
FCMB2C	CMV-driven expression construct encoding the C-terminal half of the IMPDH split intein followed by the FLNC C-terminal fragment; used in Supplementary Fig. S1B.

FCMB3C	CMV-driven expression construct encoding the C-terminal half of the Nrdj-1 split intein followed by the FLNC C-terminal fragment; used in Supplementary Fig. S1B.
FCMB4C	CMV-driven expression construct encoding the C-terminal half of the Cfa split intein followed by the FLNC C-terminal fragment; used in Supplementary Fig. S1B.
FCMB5C	CMV-driven expression construct encoding the C-terminal half of the Npu split intein followed by the FLNC C-terminal fragment; used in Supplementary Fig. S1B.
AAV-FLFLNC-N	cTnT-driven AAV transfer construct encoding the FLNC N-terminal fragment followed by the N-terminal half of the GP41-1 split intein, together with WPRE3 and a polyadenylation signal; shown in Fig. 2A.
AAV-FLFLNC-M	cTnT-driven AAV transfer construct encoding the C-terminal half of the GP41-1 split intein, followed by the FLNC middle fragment and the N-terminal half of the IMPDH split intein, together with WPRE3 and a polyadenylation signal; shown in Fig. 2A.
AAV-FLFLNC-C	cTnT-driven AAV transfer construct encoding the C-terminal half of the IMPDH split intein followed by the FLNC C-terminal fragment, together with WPRE3 and a polyadenylation signal; shown in Fig. 2A.

Supplementary Table 2. List of primers used in this study

Gene	Forward primer (5' to 3')	Reverse primer (5' to 3')
Nppa	GCTTCCAGGCCATATTGGAG	GGTGGTCTAGCAGGTTCTTG
Nppb	CTCCTATCCTCTGGGAAGTC	CCGATCCGGTCTATCTTGTG
Col1a1	AGAGCATGACCGATGGATTC	CGCTGTTCTTGCAGTGATAG
Col3a1	ATATGCCCACAGCCTTCTAC	CCACCAGTTGGACATGATTC
Gapdh	CACAGTCAAGGCCGAGAATGGGAA	GTGGTTCACACCCATCACAAACATG